



**Cationic, luminescent cyclometalated iridium(III)
complexes based on substituted 2-phenylthiazole ligands**

Journal:	<i>Dalton Transactions</i>
Manuscript ID:	DT-ART-10-2014-003054.R1
Article Type:	Paper
Date Submitted by the Author:	21-Nov-2014
Complete List of Authors:	Pope, Simon; University of Cardiff, School of Chemistry Stokes, Emily; Cardiff University, Langdon-Jones, Emily; Cardiff University, Platts, James; Cardiff University, School of Chemistry Fallis, Ian; Cardiff University, School of Chemistry; Cardiff University, Chemistry Horton, Peter; Southampton UNiversity, Chemistry Coles, Simon; Southampton, Chemistry Groves, Lara; Cardiff University, School of Chemistry

Cite this: DOI: 10.1039/c0xx00000x

www.rsc.org/xxxxxx

ARTICLE TYPE

Cationic, luminescent cyclometalated iridium(III) complexes based on substituted 2-phenylthiazole ligands

Emily C. Stokes,^a Emily E. Langdon-Jones,^a Lara M. Groves,^a James A. Platts,^a Peter N. Horton,^b Ian A. Fallis,^a Simon J. Coles^b and Simon J.A. Pope^{a*}

⁵ Received (in XXX, XXX) Xth XXXXXXXXX 20XX, Accepted Xth XXXXXXXXX 20XX
DOI: 10.1039/b000000x

Ten cationic heteroleptic iridium(III) complexes, $[\text{Ir}(\text{emptz})_2(\text{N}^{\wedge}\text{N})](\text{PF}_6)$ were prepared from a cyclometalated iridium bridged-chloride dimer involving two ethyl-4-methylphenylthiazole-5-carboxylate (emptz) ligands. One X-ray crystallographic study was undertaken where the ancillary N[^]N ligand was 4,7-diphenyl-1,10-phenanthroline and revealed the anticipated structure, showing a distorted octahedral coordination geometry at Ir(III). The complexes were visibly luminescent with modestly structured emission at 540–590 nm and lifetimes (60–340 ns) consistent with phosphorescence. TD-DFT calculations suggest that strong MLCT character contributes to the visible absorption characteristics, whilst the moderately structured emission profiles indicate a ³MLCT/³IL admixture of states to the phosphorescence.

Introduction

Cationic, cyclometalated luminescent Ir(III) (*d*⁶) complexes offer great promise in the development of photoactive components for a variety of applications.¹ For example, their use in light emitting electrochemical cells (LEECs) has been well established.² There are also interests in the use of such species as photosensitisers for visible light driven photochemical transformations including photooxidation,³ and biological imaging *via* confocal fluorescence microscopy.⁴ Recent advances in cationic Ir(III) complexes have also described piezochromic behaviour⁵ and potential application as responsive materials for data recording.⁶ From a photophysical perspective cyclometalated Ir(III) systems are very attractive due to their predictable ease of synthesis and robust (photo)chemical nature. The scope for ligand variants is huge and a great deal of effort continues to be invested in understanding the nature and interplay of excited states localised on the complex.⁷ This is particularly true when considering tuning emission wavelengths of such complexes, especially towards white light emitters, which are of great material value.⁸

The use of 2-phenylbenzothiazole type cyclometalating ligands has been well documented⁹ and has yielded a variety of important complexes for various applications. Despite yielding complexes with attractive photophysical properties, simpler phenylthiazole ligands are less well known with Ir(III).¹⁰

We are particularly interested in the development of emissive Ir(III) compounds with scope for further functionality, having previously studied Ir(III) species with tunable emission¹¹ and water solubility¹² achieved *via* peripheral groups on the cyclometalating ligands. This article describes the synthesis and characterisation of a range of luminescent Ir(III) complexes $[\text{Ir}(\text{C}^{\wedge}\text{N})_2(\text{N}^{\wedge}\text{N})](\text{PF}_6)$ that incorporate a cyclometalated 2-

phenylthiazole ligand, that is substituted with both ethyl ester and methyl groups, and incorporate a third ancillary ligand based upon different diimine-type chelates (Scheme 1).

Results and Discussion

Synthesis and characterisation of the ligands and complexes

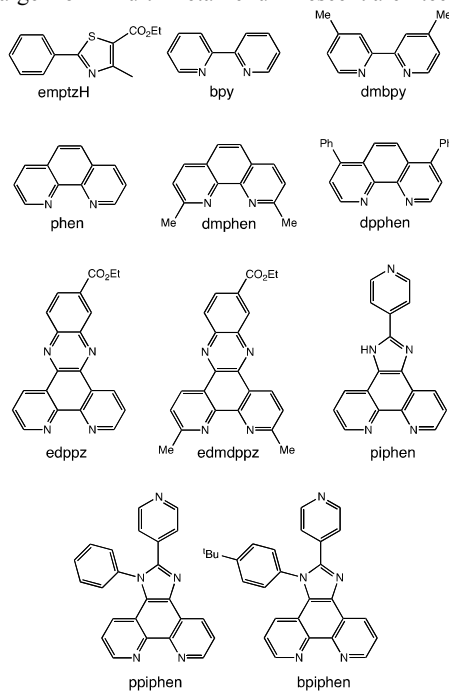
Ethyl-4-methyl-phenylthiazole-5-carboxylate (**emptzH**) was synthesised from the condensation of thiobenzamide and ethyl 4-chloroacetoacetate in ethanol. For the diimine ligands, **edppz**¹³ and **piphen**¹⁴ were synthesised according to variations on the literature methods. New ligand **edmdppz** was synthesised in an analogous manner to **edppz**, but using 2,9-dimethyl-1,10-phenanthroline-5,6-dione as the precursor. New ligands **ppiphen** and **bpiphen** were both synthesised from 1,10-phenanthroline-5,6-dione using a one-pot method and isolated in moderate yield.

The monometallic mixed ligand iridium complexes were synthesised utilising the well-established method¹⁵ of firstly isolating the dichloro-bridged dimer species followed by subsequent addition of the ancillary ligand. Thus, reaction of dimeric **1** (Scheme 2), isolated from the reaction of $\text{IrCl}_3 \cdot x\text{H}_2\text{O}$ and **emptzH**, and different diimines (N[^]N), namely 2,2'-bipyridine (**bpy**), 4,4'-dimethyl-2,2'-bipyridine (**dmbpy**), 1,10-phenanthroline (**phen**), 2,9-dimethyl-1,10-phenanthroline (**dmphen**), 4,7-diphenyl-1,10-phenanthroline (**dpphen**), ethyl-dipyrido[3,2-*a*:2',3'-*c*]phenazine-11-carboxylate (**edppz**), ethyl-3,6-dimethyl-dipyrido[3,2-*a*:2',3'-*c*]phenazine-11-carboxylate (**edmdppz**), pyridylimidazo[4,5-*f*][1,10]phenanthroline (**piphen**), 1-phenylpyridylimidazo[4,5-*f*][1,10]phenanthroline (**ppiphen**) and 1-(4-*t*-butyl)-phenylpyridylimidazo[4,5-*f*][1,10]phenanthroline (**bpiphen**), gave ten new monometallic cationic complexes of the general form $[\text{Ir}(\text{emptz})_2(\text{N}^{\wedge}\text{N})](\text{PF}_6)$. This range of diimine

Table 1 Selected bond lengths (Å) and angles (°) for $[\text{Ir}(\text{emptz})_2(\text{dpphen})](\text{PF}_6)$.

Bond length (Å) / angle (°)					
Ir(1)–N(1)	2.074(6)	C(21)–Ir(1)–C(1)	90.6(3)	C(101)–Ir(2)–C(121)	91.9(3)
Ir(1)–N(21)	2.064(6)	C(21)–Ir(1)–N(21)	79.8(3)	C(101)–Ir(2)–N(101)	80.6(3)
Ir(1)–N(41)	2.147(6)	C(1)–Ir(1)–N(21)	91.8(3)	C(121)–Ir(2)–N(101)	91.5(3)
Ir(1)–N(42)	2.145(6)	C(21)–Ir(1)–N(1)	92.7(3)	C(101)–Ir(2)–N(121)	91.0(3)
Ir(1)–C(1)	2.033(7)	C(1)–Ir(1)–N(1)	80.0(3)	C(121)–Ir(2)–N(121)	80.1(3)
Ir(1)–C(21)	2.031(8)	N(21)–Ir(1)–N(1)	168.9(2)	N(101)–Ir(2)–N(121)	168.0(3)
Ir(2)–N(101)	2.055(7)	C(21)–Ir(1)–N(42)	170.1(3)	C(101)–Ir(2)–N(142)	94.0(3)
Ir(2)–N(121)	2.087(6)	C(1)–Ir(1)–N(42)	99.3(3)	C(121)–Ir(2)–N(142)	173.1(3)
Ir(2)–N(141)	2.149(6)	N(21)–Ir(1)–N(42)	100.0(2)	N(101)–Ir(2)–N(142)	85.9(3)
Ir(2)–N(142)	2.146(6)	N(1)–Ir(1)–N(42)	88.7(2)	N(121)–Ir(2)–N(142)	103.3(2)
Ir(2)–C(101)	2.016(8)	C(21)–Ir(1)–N(41)	93.0(3)	C(101)–Ir(2)–N(141)	170.7(3)
Ir(2)–C(121)	2.025(7)	C(1)–Ir(1)–N(41)	175.2(3)	C(121)–Ir(2)–N(141)	97.3(3)
		N(21)–Ir(1)–N(41)	85.8(2)	N(101)–Ir(2)–N(141)	100.3(3)
		N(1)–Ir(1)–N(41)	102.9(2)	N(121)–Ir(2)–N(141)	89.4(2)
		N(42)–Ir(1)–N(41)	77.1(2)	N(142)–Ir(2)–N(141)	76.9(2)
		C(21)–Ir(1)–C(1)	90.6(3)	C(101)–Ir(2)–C(121)	91.9(3)

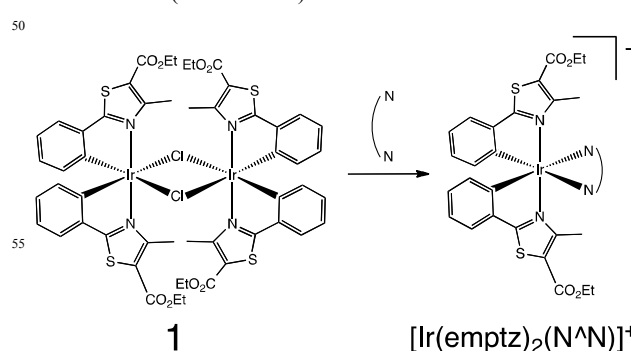
ligands (Scheme 1) was selected to study the potential influence on the electronic properties of the complexes as well as provide opportunities for further chemistry. For example, **piphen**, **ppiphen** and **bpiphen** all possess an additional pyridine coordination site, which could be utilised for further reactivity towards larger-form multi-metallic luminescent architectures.

**Scheme 1.** Ligands used in this study.

All new complexes were characterised using a range of spectroscopic techniques. The ^1H NMR spectra of the complexes show aromatic regions with overlapping resonances associated with the cyclometalated **emptz** and diimine ligands. In three examples, additional resonances were noted in the aliphatic region and attributed to transesterification with 2-methoxyethanol. Such an observation has been noted before¹² and is attributed to the reaction conditions and solvent utilised for the

complexation: the 2-methoxyethyl groups of $[\text{Ir}(\text{emptz})_2(\text{edppz})](\text{PF}_6)$, $[\text{Ir}(\text{emptz})_2(\text{piphen})](\text{PF}_6)$ and $[\text{Ir}(\text{emptz})_2(\text{ppiphen})](\text{PF}_6)$ appeared as broadened triplets around 4.5 and 3.7 ppm together with a singlet *ca.* 3.3 ppm.

Both low and high resolution mass spectra were obtained for the complexes revealing the parent cations of $[\text{M}(\text{PF}_6)]^+$, with the appropriate isotopic distribution for each case. Solid-state IR spectra were also obtained on all complexes highlighting the ester functionality (*ca.* 1720 cm^{-1}) and the hexafluorophosphate counter anion (*ca.* 835 cm^{-1}).

**Scheme 2.** Synthesis of the complexes.

60 X-ray crystallography studies

Single crystals of $[\text{Ir}(\text{emptz})_2(\text{dpphen})](\text{PF}_6)$ were isolated from vapour diffusion of Et_2O into concentrated CHCl_3 solution of the complex over a period of 48 h at -20°C , and found to be suitable for X-ray diffraction studies. The bond lengths and bond angles for $[\text{Ir}(\text{emptz})_2(\text{dpphen})](\text{PF}_6)$ are reported in Table 1, and the associated data collection parameters are reported in Table S1, electronic supplementary information (ESI).

The structure (Figure 1) confirmed the proposed formulation, and showed that the Ir(III) ion in this complex adopts a distorted octahedral coordination geometry. The bond lengths are typical of this complex type.¹¹ The *trans* angles at the metal ion range from 168.0(3)° to 175.2(3)° for $[\text{Ir}(\text{emptz})_2(\text{dpphen})]^+$. As expected the diimine ligand was coordinated *trans* to the

cyclometalated phenyl rings and the complex retains the *cis*-C,C and *trans*-N,N chelating arrangement of the original chloro-bridged dimer. The Ir-N bond lengths for the diimine ligand are longer than the **emptz** ligands. The structure of **[Ir(emptz)₂(dpphen)]⁺** also revealed that the phenyl substituents of the dpphen ligand were twisted out of planarity from the phenanthroline unit by *ca.* 56°.

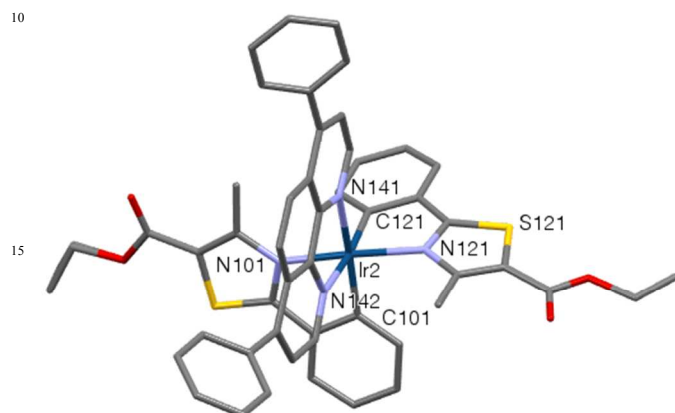


Figure 1. Structural representation of **[Ir(emptz)₂(dpphen)]⁺**. Just one of the crystallographically different moieties is shown with the solvent molecules, PF₆⁻ anion and hydrogen atoms omitted for clarity.

Density Functional Theory (DFT) studies

DFT calculations (computed using the B3LYP hybrid functional) were performed to investigate the electronic absorption bands of **[Ir(emptz)₂(phen)]⁺** and the orbitals involved in these. The crystal structure illustrated in Figure 1 was truncated by replacement of phen-based Ph groups with H, and the resulting cation's structure optimized. Absorption bands at this optimal geometry were then calculated using scalar relativistic TD-DFT in a simulated acetonitrile environment, and are reported in Table 2. These data predict the lowest energy band at 450 nm to be very weak, but that a stronger band exists at 444 nm. This band is dominated by excitation of an electron from the HOMO to LUMO+1: analysis of MO coefficients indicates that the HOMO has significant 5*d* character (23.5%), while LUMO+1 is almost exclusively located on the thiazole rings (1.7% 5*d* character).

Table 2 Calculated absorption wavelengths for **[Ir(emptz)₂(phen)]⁺** from TD-DFT studies.

λ (nm) ^a	f ^b	character	λ (nm)	f	Character
450	0.0002	HOMO → LUMO	365	0.1135	HOMO-1 → LUMO+2
444	0.159	HOMO → LUMO+1	355	0.0003	HOMO-2 → LUMO+1
435	0.0001	HOMO → LUMO+2	348	0.0541	HOMO-2 → LUMO+2
405	0.0469	HOMO → LUMO+3	345	0.0367	HOMO-2 → LUMO+3
371	0.0584	HOMO-1 → LUMO	344	0.0385	HOMO-1 → LUMO+3
367	0.0116	HOMO-1 → LUMO+1	339	0.0151	HOMO-4 → LUMO

^a absorption wavelength; ^b oscillator strength.

Thus, we assign this band as having strong MLCT character, but in this case the ligand in question is the phenylthiazole. The more typical excitation of a 5*d* electron into the π^* MO on phen (which is the LUMO here) is possible, but is either weak (450 nm) or high energy (371 nm). Figure S1 (ESI) shows the diagrammatical representation of the calculated HOMO-1, HOMO and LUMO. The calculated HOMO-LUMO energy gap of 3.43 eV compared closely to that reported (3.32 eV) for **[Ir(ppy)₂(bpy)]⁺** (where ppy = 2-phenylpyridine).^{1a}

Electrochemical studies

The electrochemical characteristics of the **[Ir(emptz)₂(N[^]N)](PF₆)** complexes were studied in deoxygenated CH₂Cl₂. The cyclic voltammograms, measured at a platinum disc electrode (scan rate $\nu = 200 \text{ mV s}^{-1}$, $1 \times 10^{-3} \text{ M}$ solutions, 0.1 M [NBu₄][PF₆] as a supporting electrolyte), each (for example, Figures S2 and S3 in the ESI) generally showed one non-fully reversible oxidation around +1.55 V, which was assigned to the Ir^{3+/4+} couple. The comparative potential for **[Ir(ppy)₃]** is +1.0 V/NHE.¹⁶ Related cationic complexes, recorded under identical conditions, that incorporate cyclometalated cinchophen-type ligands¹² **[Ir(epqc)₂(bpy)](PF₆)** (where epqc = ethyl-2-phenylquinoline-4-carboxylate) possess a Ir^{3+/4+} couple around +1.40 V. Therefore these results clearly suggest that the Ir(III) ion is relatively stabilised in the **emptz** variants versus **epqc**. The complexes also showed fully reversible (for the **bpy**, **phen**, **dpphen**, **ppiphen**, **edmdppz**) or quasi-reversible (**dmbpy**, **dmpphen**, **piphen**, **edppz**, **bpiphen**) reduction waves. The former were assigned to ligand-centred processes involving the diimine whilst the latter may include contributions from the phenylthiazole ligands. The cyclic voltammetry of **[Ir(ppy)₂(bpy)]⁺** has been reported to show quasi-reversible waves (in acetonitrile *versus* SCE) at +1.32 and -1.40 V,¹⁷ the former attributed to the Ir^{3+/4+} couple.¹⁸

Electronic properties: UV-vis and luminescence data

The UV-vis absorption spectra of the complexes were recorded as aerated MeCN solutions (10⁻⁵ M) (Figure 2, Table 3). Strong absorption bands between 200 and 400 nm were assigned to the various spin allowed ¹ π - π^* ligand-centred transitions arising from both the cyclometalated and diimine ligands of the complexes. Both dppz-derived species show additional bands at 370 and 390 nm, which are attributed to the extended conjugation of the fused chromophore. Slightly weaker bands ($\epsilon \sim 7000 \text{ M}^{-1}\text{cm}^{-1}$) at 400-475 nm were assigned to spin-allowed metal-to-ligand charge

Table 3 Photophysical and redox properties of the $[\text{Ir}(\text{emtpz})_2(\text{N}^{\wedge}\text{N})]\text{PF}_6$ complexes.

Complex	E/V^a	$\lambda_{\text{abs}} (\text{nm})^b$	$\lambda_{\text{em}} / \text{nm}^{b,c}$	$\lambda_{\text{em}} / \text{nm}^c (77\text{K})$	$\tau / \text{ns}^{b,d}$	ϕ^b
$[\text{Ir}(\text{emtpz})_2(\text{bpy})]\text{PF}_6$	+1.56, -1.33	269 (26000), 305 (35200), 370 (7000), 442 (6700)	549, 586 sh	538, 558, 582, 604 sh, 634, 656 sh	282	0.014
$[\text{Ir}(\text{emtpz})_2(\text{dmbpy})]\text{PF}_6$	+1.51, -1.43	267 (26200), 305 (34400), 369 (8000), 446 (7000)	549, 588 sh	540, 559, 583, 606 sh, 635, 659 sh	260	0.012
$[\text{Ir}(\text{emtpz})_2(\text{phen})]\text{PF}_6$	+1.53, -1.35	272 (47700), 297 (35100), 317 (29200), 368 (9400), 439 (7400)	549, 586 sh	541, 559, 586, 608 sh, 633 sh, 658 sh	270	0.012
$[\text{Ir}(\text{emtpz})_2(\text{dmphen})]\text{PF}_6$	+1.59, -1.46	283 (35100), 369 (9400), 435 (5700)	554, 593 sh	545, 564, 590, 614 sh, 642 sh	308	0.011
$[\text{Ir}(\text{emtpz})_2(\text{dpphen})]\text{PF}_6$	+1.53, -1.30	289 (53800), 368 (13500), 435 (8100)	549, 587 sh	538, 558, 582, 601, 631, 658 sh	269	0.015
$[\text{Ir}(\text{emtpz})_2(\text{edppz})]\text{PF}_6$	+1.54, -1.29	282 (10100), 367 (21800), 389 (17800), 437 (8800)	550, 594 sh	539, 556, 582, 604 sh, 632, 659 sh	60	0.0003
$[\text{Ir}(\text{emtpz})_2(\text{edmdppz})]\text{PF}_6$	+1.67, -0.81	283 (93900), 369 (21600), 388 (18200), 436 (7600)	557, 595sh	559, 601, 659	184	0.002
$[\text{Ir}(\text{emtpz})_2(\text{piphen})]\text{PF}_6$	+1.57, -1.16	280 (67000), 318 (47300), 367 (14500), 435 (9300)	549, 586 sh	542, 558, 584, 606sh, 632 sh, 658 sh	257	0.012
$[\text{Ir}(\text{emtpz})_2(\text{ppiphen})]\text{PF}_6$	+1.53, -1.30	282 (66700), 371 (11900), 397 (9000), 439 (8600)	550, 587 sh	538, 558, 582, 603, 631, 659 sh	340	0.015
$[\text{Ir}(\text{emtpz})_2(\text{bpiphen})]\text{PF}_6$	+1.58, -1.30	282 (71200), 371 (12100), 398 (9200), 440 (8600)	548, 586 sh	537, 558, 581, 604 sh, 632, 657 sh	286	0.012

^a potentials measured in CH_2Cl_2 solutions at 200 mV s^{-1} with 0.1 M $[\text{NBu}_4][\text{PF}_6]$ as supporting electrolyte calibrated with Fc/Fc^+ . ^b MeCN, room temperature solution; ^c $\lambda_{\text{exc}} = 380 \text{ nm}$; ^d $\lambda_{\text{exc}} = 372 \text{ nm}$.

transfer bands ($^1\text{MLCT}$). These correlate remarkably well with the absorption band at 444 nm calculated using TD-DFT, and thus lend support to the theoretical methodology used. For complexes of the dppz derivatives and arylimidazo[4,5-*f*][1,10]phenanthroline-type ligands, $n-\pi^*$ transitions should also be present, albeit at lower molar absorption coefficients that may preclude their observation. The coordinated $\text{N}^{\wedge}\text{N}$ ligand imparts little influence on the energy of the $^1\text{MLCT}$ transition, an observation that may be explained by the TD-DFT prediction that the absorption *ca.* 445 nm predominantly involves the phenylthiazole, rather than the $\text{N}^{\wedge}\text{N}$ ligand.

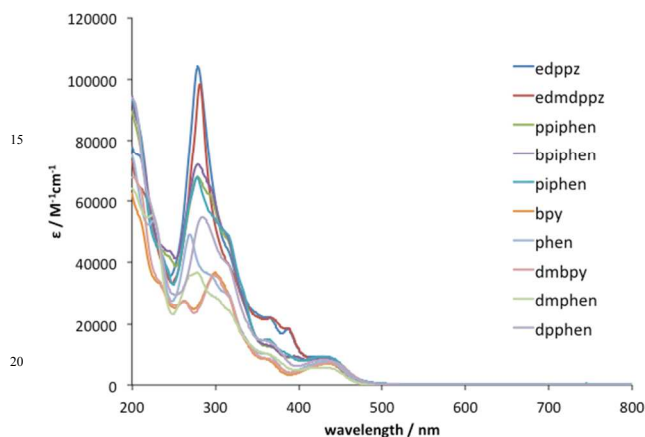


Figure 2. UV-vis spectra for $[\text{Ir}(\text{emtpz})_2(\text{N}^{\wedge}\text{N})]\text{PF}_6$ complexes in MeCN solutions (10^{-5} M).

For $[\text{Ir}(\text{emtpz})_2(\text{phen})](\text{PF}_6)$, the collected absorption and electrochemical data for this complex were utilised to determine $E_{\text{HOMO}} = -5.87 \text{ eV}$, $E_{\text{LUMO}} = -3.31 \text{ eV}$ (where $-E_{\text{HOMO}} = E_{\text{ox}} - E_{\text{Fc}/\text{Fc}^+} + 4.8$) and $E_{\text{bandgap}} = 2.56 \text{ eV}$. The DFT calculated values for E_{HOMO} and E_{LUMO} were -6.06 eV and -2.63 eV respectively, with a resultant calculated E_{bandgap} of 3.43 eV , suggesting that DFT overestimates the level of the LUMO; a similar observation

has been noted previously for $[\text{Ir}(\text{ppy})_2(\text{bpy})]^+$.^{1a}

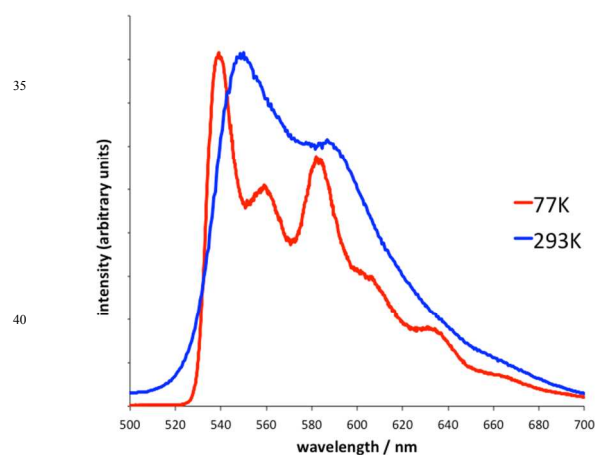


Figure 3. Normalised emission spectra of $[\text{Ir}(\text{emtpz})_2(\text{dpphen})]\text{PF}_6$ obtained at 293K (MeCN) and 77K (EtOH/MeOH glass).

The room temperature solution state emission spectra (Table 3) for all of the complexes showed visible luminescence around 550 nm with a low energy shoulder at *ca.* 586 nm (for comparison $[\text{Ir}(\text{ppy})_2(\text{bpy})]^+$ emits at 602 nm in MeCN from a mixed $^3\text{LLCT}/^3\text{MLCT}$ excited state).^{1a} These results are also in line with $[\text{Ir}(\text{C}^{\wedge}\text{N})_2(\text{bpy})](\text{PF}_6)$ (where $\text{C}^{\wedge}\text{N} = 4\text{-methyl-2-phenylthiazole}$) which has a reported emission at 584 nm and has been successfully utilised as a photosensitiser for hydrogen generation from water.^{10b} Importantly, the emission characteristics are retained across the entire range of different functionalised diimine ligands, with minor variations in λ_{em} observed according to ligand type. The emission lifetimes were obtained in aerated solvent and were typically in the range 180-340 ns, which is consistent with an emitting state of triplet character. The quantum yields were obtained using aerated MeCN solutions and were typically between 1-2%. This is comparable to the cationic cinchophen Ir(III) complexes described in related studies.¹² The

quantum yield for $[\text{Ir}(\text{ppy})_2(\text{bpy})](\text{PF}_6)$ is higher at *ca.* 9% but was obtained using degassed MeCN.¹⁹

Low temperature emission spectra of each complex were also obtained on MeOH/EtOH (1:1) glasses and revealed a highly structured emission profile. When compared to the room temperature measurements (Figure 3) it is clear that the spectra share key features. The vibronically structured spectra suggest a significant ligand-centred triplet component (attributed to the phenylthiazole ligand) to the emitting state at 77K, which also contributes at room temperature.

The comparative room temperature data for the dppz-type complexes $[\text{Ir}(\text{emptz})_2(\text{edppz})]\text{PF}_6$ and $[\text{Ir}(\text{emptz})_2(\text{edmdppz})]\text{PF}_6$ revealed shorter lifetimes (60 and 184 ns) and lower quantum yields (< 0.002%) which were indicative of quenching processes. Further investigation using low temperature measurements (Figure 4) showed that the triplet states of the free dppz ligands must lie in close proximity to the emitting state of the complexes, which has been noted in studies using Re(I) complexes.²⁰ Barton has previously reported the related complex $[\text{Ir}(\text{ppy})_2(\text{edppz})]\text{Cl}$ to be non-emissive in MeCN, although $[\text{Ir}(\text{ppy})_2(\text{dppz})]\text{Cl}$ emits at 634 nm, which is clearly a lower energy than the **emptz** species described here.¹³ Therefore it is likely that in MeCN at room temperature quenching pathways *via* dppz-localised excited states are operable in these two complexes.

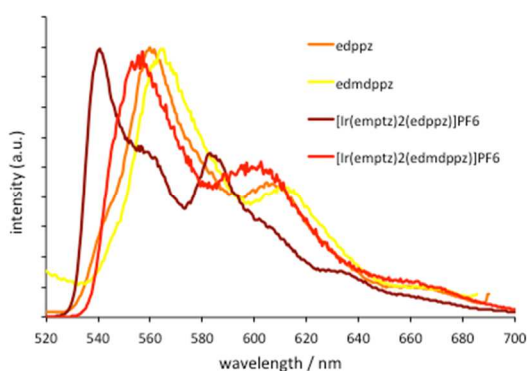


Figure 4. Normalised 77K emission spectra of $[\text{Ir}(\text{emptz})_2(\text{edppz})]\text{PF}_6$ and $[\text{Ir}(\text{emptz})_2(\text{edmdppz})]\text{PF}_6$ and corresponding free ligands.

Experimental Section

All reactions were performed with the use of vacuum line and Schlenk techniques. Reagents were commercial grade and used without further purification. ^1H and $^{13}\text{C}\{-^1\text{H}\}$ NMR spectra were recorded on an NMR-FT Bruker 400 or 250 MHz and $^{31}\text{P}\{-^1\text{H}\}$ NMR spectra on a Joel Eclipse 300 MHz spectrometer and recorded in CDCl_3 or MeOD solutions. ^1H and $^{13}\text{C}\{-^1\text{H}\}$ NMR chemical shifts (δ) were determined relative to internal tetramethylsilane, $\text{Si}(\text{CH}_3)_4$ and are given in ppm. Low-resolution mass spectra (LRMS) were obtained by the staff at Cardiff University. High-resolution mass spectra (HRMS) were carried out at the EPSRC National Mass Spectrometry Service at Swansea University, UK. UV-Vis studies were performed on a Jasco V-650 spectrophotometer fitted with a Jasco temperature control unit in MeCN or MeOH solutions (10^{-5} M) at 20 °C. Photophysical data were obtained on a JobinYvon–Horiba

Fluorolog spectrometer fitted with a JY TBX picoseconds photodetection module in MeCN, MeOH or H_2O solutions.

Emission spectra were uncorrected and excitation spectra were instrument corrected. The pulsed source was a Nano-LED configured for 372 or 459 nm output operating at 500 kHz. Luminescence lifetime profiles were obtained using the JobinYvon–Horiba FluoroHub single photon counting module and the data fits yielded the lifetime values using the provided DAS6 deconvolution software. Electrochemical studies were carried out using a Parstat 2273 potentiostat in conjunction with a three-electrode cell. The auxiliary electrode was a platinum wire and the working electrode a platinum (1.0 mm diameter) disc. The reference was a silver wire separated from the test solution by a fine porosity frit and an agar bridge saturated with KCl. Solutions (10 ml CH_2Cl_2) were 1.0×10^{-3} mol dm^{-3} in the test compound and 0.1 mol dm^{-3} in $[\text{NBu}_4][\text{PF}_6]$ as the supporting electrolyte. Under these conditions, E^0 , for the one-electron oxidation of $[\text{Fe}(\eta\text{-C}_5\text{H}_5)_2]$ added to the test solutions as an internal calibrant, is +0.46 V in CH_2Cl_2 .²¹ Unless specified, all electrochemical values are at $v = 200$ mV s^{-1} .

Crystallography

Suitable crystals were selected and measured following a standard method²² on a Rigaku AFC12 goniometer equipped with an enhanced sensitivity (HG) Saturn724+ detector mounted at the window of a FR-E+ SuperBright molybdenum rotating anode generator with VHF Varimax optics (70 μm focus) at 100K. Cell determination, data collection, reduction, cell refinement and absorption correction carried out using CrystalClear-SM Expert 3.1b27.²³ Structures solved using SUPERFLIP²⁴ and refined using SHELXL-2013.²⁵

For $[\text{Ir}(\text{emptz})_2(\text{dpphen})](\text{PF}_6)$ there is a molecule of ether disordered over the inversion centre, along with a disordered ethoxy group. As such various geometrical and displacement restraints and constraints were employed.

CCDC reference number 1025666 $[\text{Ir}(\text{emptz})_2(\text{dpphen})]\text{PF}_6$, contains the supplementary crystallographic data for this paper. These data can be obtained free of charge from the Cambridge Crystallographic Data Centre *via* www.ccdc.cam.ac.uk/data_request/cif.

DFT studies

DFT geometry optimisation and orbital calculations were performed on the Gaussian09 program.²⁶ Geometry optimisations were carried out without constraints using the B3LYP functional. The Stuttgart-Dresden²⁷ basis set and effective core potential was used for Ir centre, along with 6-31G(d)²⁸ basis set for all remaining atoms. TD-DFT studies were performed in Gaussian09²⁹ using the same functional, but with 6-31+G(d,p) on all non-metal atoms, and also included a simulated MeCN environment using the polarised continuum model (PCM) approach.³⁰

Synthesis

Ethyl-4-methyl-2-phenylthiazole-5-carboxylate (emptzH),³¹ 1,10-phenanthroline-5,6-dione,³² 2,9-dimethyl-1,10-phenanthroline-5,6-dione,³³ ethyl-3,4-diaminobenzoate,³⁴ ethyl-dipyrido[3,2-*a*:2',3'-*c*]phenazine-11-carboxylate (edppz),³⁵ pyridylimidazo[4,5-*f*][1,10]phenanthroline (piphen),¹⁴ were

synthesised according to the literature methods or subtle variations thereupon.

[Ir(emptz)₂(μ-Cl)₂Ir(emptz)₂] **1** was prepared *via* a variation of the standard literature procedures for chloro-bridged dimers: IrCl₃·xH₂O (0.214 g, 0.15 mmol) was dissolved in 2-methoxyethanol (6 mL) and water (2 mL), **emptzH** (0.353 g, 1.43 mmol) was added and the solution stirred at 120 °C for 48 h. Water (approx. 20 mL) was added to give a bright orange precipitate. The product was used in subsequent reactions without further purification. Yield: 0.481 g, 94%.

[Ir(emptz)₂(bpy)]PF₆

1 (0.165 g, 0.11 mmol) and 2,2'-bipyridine (0.046 g, 0.29 mmol) in 2-methoxyethanol (5 mL) were heated at 120 °C for 16 h. The solvent was then removed *in vacuo* and the crude product dissolved in MeCN (4 mL). KPF₆ (1 g, 5.43 mmol) in water (2 mL) was added and the solution stirred for approx. 10 mins. Water (approx. 20 mL) was added and the product extracted with CH₂Cl₂ (2 × 20 mL). The combined organic phases were washed with water and dried over MgSO₄. The solution was filtered and the solvent removed *in vacuo*. The crude product was then purified by column chromatography (silica, CH₂Cl₂). After elution of unreacted organics with CH₂Cl₂ the product was eluted as the only orange fraction with CH₂Cl₂/MeOH (9:1). The product was concentrated in volume (*ca.* 3 mL), precipitated by the slow addition of Et₂O and dried *in vacuo*. Yield: 0.145 g, 64%. ¹H NMR (400 MHz, CDCl₃): δ_H = 9.33 (2H, d, ³J_{HH} = 8.2 Hz), 8.85 (2H, app. dt, J_{HH} = 7.9, 1.4 Hz), 8.56 (2H, app. dd, J_{HH} = 1.0, 5.6 Hz), 8.38 (2H, dd, J_{HH} = 0.9, 7.7 Hz), 8.18-8.14 (2H, m), 7.76 (2H, app. dt, J_{HH} = 0.9, 17.4 Hz), 7.66 (2H, app. dt, J_{HH} = 7.6, 1.3 Hz), 7.10 (2H, d, ³J_{HH} = 7.5 Hz), 4.98 (4H, q, ³J_{HH} = 7.1 Hz, OCH₂CH₃), 2.49 (6H, s, CCH₃), 2.00 (6H, t, ³J_{HH} = 7.1 Hz, OCH₂CH₃) ppm. UV-Vis (CH₃CN): λ_{max}/nm (ε/M⁻¹cm⁻¹) = 442 (6700), 370 (7000), 305 (35200), 269 (26000). LRMS (ES⁺) found *m/z* 841.00; calculated 841.01 for [M-PF₆]⁺. HRMS (ES⁺) found *m/z* 841.1478; calculated 841.1487 for [C₃₆H₃₂N₄O₄S₂Ir]⁺. IR (solid): ν 1719 (C=O), 1256, 1244 (C-O), 835 (PF₆⁻) cm⁻¹.

[Ir(emptz)₂(dmbpy)]PF₆

As for **[Ir(emptz)₂(bpy)]PF₆**, but using **1** (0.08 g, 0.06 mmol) and 4,4'-dimethyl-2,2'-bipyridine (0.026 g, 0.14 mmol). The crude product was purified by column chromatography (silica, CH₂Cl₂). After elution of unreacted organics with CH₂Cl₂ the product was eluted as the only orange fraction with CH₂Cl₂/MeOH (9:1). Yield: 0.039 g, 35%. ¹H NMR (400 MHz, CDCl₃): δ_H = 8.55 (2H, s), 7.64 (2H, app. d, ³J_{HH} = 7.2 Hz), 7.59 (2H, d, ³J_{HH} = 5.6 Hz), 7.12 (2H, d, ³J_{HH} = 5.4 Hz), 7.04-7.00 (2H, m), 6.93-6.89 (2H, m), 6.36 (2H, d, ³J_{HH} = 7.6 Hz), 4.26 (4H, q, ³J_{HH} = 7.1 Hz, OCH₂CH₃), 2.57 (6H, s, CH₃), 1.79 (6H, s, CH₃), 1.28 (6H, t, ³J_{HH} = 7.1 Hz, OCH₂CH₃) ppm. UV-Vis (CH₃CN): λ_{max}/nm (ε/M⁻¹cm⁻¹) = 446 (7000), 369 (8000), 305 (34400), 267 (26200). LRMS (ES⁺) found *m/z* 869.24; calculated 869.08 for [M-PF₆]⁺. HRMS (ES⁺) found *m/z* 869.1795; calculated 869.1801 for [C₃₈H₃₆N₄O₄S₂Ir]⁺. IR (solid): ν 1716 (C=O), 1253, 1242 (C-O), 824 (PF₆⁻) cm⁻¹.

[Ir(emptz)₂(phen)]PF₆

As for **[Ir(emptz)₂(bpy)]PF₆**, but using **1** (0.049 g, 0.03 mmol) and 1,10-phenanthroline (0.014 g, 0.08 mmol). The crude product was purified by column chromatography (silica, CH₂Cl₂). After elution of unreacted organics with CH₂Cl₂ the product was eluted as the only orange fraction with CH₂Cl₂/MeOH (9:1). Yield: 0.035 g, 51%. ¹H NMR (400 MHz, CDCl₃): δ_H = 8.68 (2H, app. dd, J_{HH} = 8.3, 1.3 Hz), 8.18 (2H, s), 8.15 (2H, app. dd, J_{HH} = 5.1, 1.3 Hz), 7.83 (2H, app. dd, J_{HH} = 8.2, 5.1 Hz), 7.71 (2H, app. dd, J_{HH} = 7.7, 0.9 Hz), 7.12-7.07 (2H, m), 7.00-6.96 (2H, m), 6.48 (2H, d, ³J_{HH} = 7.5 Hz), 4.19 (4H, q, ³J_{HH} = 7.1 Hz, OCH₂CH₃), 1.48 (6H, s, CH₃), 1.14 (6H, t, ³J_{HH} = 7.0 Hz, OCH₂CH₃) ppm. UV-Vis (CH₃CN): λ_{max}/nm (ε/M⁻¹cm⁻¹) = 439 (7400), 368 (9400), 317 (29200), 297 (35100), 272 (47700), 229 (52400). LRMS (ES⁺) found *m/z* 865.15; calculated 865.05 for [M-PF₆]⁺. HRMS (ES⁺) found *m/z* 865.1482; calculated 865.1488 for [C₃₈H₃₂N₄O₄S₂Ir]⁺. IR (solid): ν 1719 (C=O), 1256, 1244 (C-O) 833 (PF₆⁻) cm⁻¹.

[Ir(emptz)₂(dmphen)]PF₆

As for **[Ir(emptz)₂(bpy)]PF₆**, but using **1** (0.080 g, 0.06 mmol) and 2,9-dimethyl-1,10-phenanthroline (0.036 g, 0.17 mmol). The crude product was purified by column chromatography (silica, CH₂Cl₂). After elution of unreacted organics with CH₂Cl₂ the product was eluted as the only orange fraction with CH₂Cl₂/MeOH (9:1). Yield: 0.053 g, 46%. ¹H NMR (400 MHz, CDCl₃): δ_H = 8.49 (2H, d, ³J_{HH} = 8.3 Hz), 8.01 (2H, s), 7.58 (2H, d, ³J_{HH} = 8.9 Hz), 7.54 (2H, d, ³J_{HH} = 6.9 Hz), 6.39 (2H, app. t, ³J_{HH} = 7.2 Hz), 6.80 (2H, app. dt, J_{HH} = 7.5, 1.1 Hz), 6.18 (2H, d, ³J_{HH} = 7.7 Hz), 4.23 (4H, q, ³J_{HH} = 7.1 Hz, OCH₂CH₃), 2.08 (6H, s, CH₃), 1.50 (6H, s, CH₃), 1.14 (6H, t, ³J_{HH} = 7.0 Hz, OCH₂CH₃) ppm. UV-Vis (CH₃CN): λ_{max}/nm (ε/M⁻¹cm⁻¹) = 435 (5700), 369 (9400), 283 (35100), 228 (53800). LRMS (ES⁺) found *m/z* 893.22; calculated 893.10 for [M-PF₆]⁺. HRMS (ES⁺) found *m/z* 893.1797; calculated 893.1801 for [C₄₀H₃₆N₄O₄S₂Ir]⁺. IR (solid): ν 1717 (C=O), 1093 (C-O), 837 (PF₆⁻) cm⁻¹.

[Ir(emptz)₂(dpphen)]PF₆

As for **[Ir(emptz)₂(bpy)]PF₆**, but using **1** (0.080 g, 0.06 mmol) and 4,7-diphenyl-1,10-phenanthroline (0.041 g, 0.12 mmol). The crude product was purified by column chromatography (silica, CH₂Cl₂). After elution of unreacted organics with CH₂Cl₂ the product was eluted as the only orange fraction with CH₂Cl₂/MeOH (9:1). Yield: 0.084 g, 65%. ¹H NMR (400 MHz, CDCl₃): δ_H = 8.22 (2H, d, ³J_{HH} = 5.3 Hz), 8.12 (2H, s), 7.75-7.71 (4H, m), 7.55-7.50 (10H, m), 7.12-7.08 (2H, m), 7.02-6.98 (2H, m), 6.51 (2H, d, ³J_{HH} = 7.6 Hz), 4.22 (4H, q, ³J_{HH} = 7.1 Hz, OCH₂CH₃), 1.66 (6H, s, CH₃), 1.25 (6H, t, ³J_{HH} = 7.1 Hz, OCH₂CH₃) ppm. UV-Vis (CH₃CN): λ_{max}/nm (ε/M⁻¹cm⁻¹) = 435 (8100), 368 (13500), 289 (53800). LRMS (ES⁺) found *m/z* 1017.30; calculated 1017.25 for [M-PF₆]⁺. HRMS (ES⁺) found *m/z* 1017.2111; calculated 1017.2115 for [C₅₀H₄₀N₄O₄S₂Ir]⁺. IR (solid): ν 1707 (C=O), 1258, 1246 (C-O), 835 (PF₆⁻) cm⁻¹.

[Ir(emptz)₂(edppz)]PF₆

As for **[Ir(emptz)₂(bpy)]PF₆**, but using **1** (0.052 g, 0.04 mmol) and **edppz** (0.029 g, 0.08 mmol). The crude product was purified by column chromatography (silica, CH₂Cl₂). After elution of unreacted organics with CH₂Cl₂ the product was eluted as the

third orange fraction with CH₂Cl₂/MeOH (99:1). Yield: 0.018 g, 20%. ¹H NMR (250 MHz, CDCl₃): δ_H = 9.84-9.80 (2H, m), 9.07 (1H, app. d, ³J_{HH} = 1.2 Hz), 8.51-8.50 (1H, m), 8.45 (1H, d, ³J_{HH} = 9.0 Hz), 8.28 (2H, d, ³J_{HH} = 5.1 Hz), 8.05-8.00 (2H, m), 7.75-7.72 (2H, m), 7.14-7.00 (4H, m), 6.49 (2H, d, ³J_{HH} = 7.6 Hz), 4.45 (2H, q, ³J_{HH} = 7.1 Hz, OCH₂CH₃), 4.27-4.24 (4H, m, OCH₂CH₂OCH₃), 3.54-3.50 (4H, m, OCH₂CH₂OCH₃), 3.24 (6H, s, OCH₃), 1.64 (6H, s, CH₃) 1.44 (3H, t, ³J_{HH} = 7.1 Hz, OCH₂CH₃) ppm. UV-Vis (CH₃CN): λ_{max}/nm (ε/M⁻¹cm⁻¹) = 437 (8800), 389 (17800), 367 (21800), 282 (10100). LRMS (ES⁺) found *m/z* 1099.24; calculated 1099.26 for [M-PF₆]⁺. HRMS (ES⁺) found *m/z* 1099.2115; calculated 1099.2129 for [C₄₉H₄₂N₆O₈S₂Ir]⁺. IR (solid): ν 1707 (C=O), 1244 (C-O), 833 (PF₆⁻) cm⁻¹.

[Ir(emptz)₂(edmdppz)]PF₆

As for [Ir(emptz)₂(bpy)]PF₆, but using **1** (0.051 g, 0.035 mmol) and **edmdppz** (0.031 g, 0.081 mmol). The crude product was purified by column chromatography (silica, CH₂Cl₂). After elution of unreacted organics with CH₂Cl₂ the product was eluted as the first yellow fraction with CH₂Cl₂. Yield: 0.026 g, 30%. ¹H NMR (400 MHz, CDCl₃): δ_H = 9.78 (2H, dd, *J*_{HH} = 8.3, 6.5 Hz), 9.06 (1H, s), 8.51 (1H, dd, *J*_{HH} = 9.0, 1.8 Hz), 8.41 (1H, d, ³J_{HH} = 9.0 Hz), 7.86 (2H, dd, *J*_{HH} = 8.4, 3.8 Hz), 7.56 (2H, d, ³J_{HH} = 7.7 Hz), 6.97-6.93 (2H, m), 6.84-6.81 (2H, m), 6.21 (2H, d, ³J_{HH} = 7.8 Hz), 4.47 (2H, q, ³J_{HH} = 7.1 Hz, OCH₂CH₃), 4.19 (4H, q, ³J_{HH} = 7.1 Hz, OCH₂CH₃), 2.14 (6H, s, CH₃), 1.72 (6H, s, CH₃), 1.45 (3H, t, ³J_{HH} = 7.1 Hz, OCH₂CH₃), 1.20 (3H, t, ³J_{HH} = 7.9 Hz, OCH₂CH₃) ppm. UV-Vis (CH₃CN): λ_{max}/nm (ε/M⁻¹cm⁻¹) = 436 (7600), 388 (18200), 369 (21600), 283 (93900). LRMS (ES⁺) found *m/z* 1067.23; calculated 1067.26 for [M-PF₆]⁺. HRMS (ES⁺) found *m/z* 1067.2115; calculated 1067.2231 for [C₄₉H₄₂N₆S₂O₆Ir]⁺. IR (solid): ν 1713 (C=O), 1257, 1244 (C-O), 829 (PF₆⁻) cm⁻¹.

[Ir(emptz)₂(piphen)]PF₆

As for [Ir(emptz)₂(bpy)]PF₆, but using **1** (0.051 g, 0.04 mmol) and **piphen** (0.026 g, 0.09 mmol). The crude product was purified by column chromatography (silica, CH₂Cl₂). After elution of unreacted organics with CH₂Cl₂ the product was eluted as the first yellow fraction with CH₂Cl₂/MeOH (99:1). Yield: 0.034 g, 41%. ¹H NMR (400 MHz, CDCl₃): δ_H = 9.14 (2H, app. t, ³J_{HH} = 7.9 Hz), 8.90-8.74 (2H, br. s), 8.26-8.22 (4H, m), 8.03-8.00 (1H, m), 7.96-7.92 (1H, m), 7.72 (2H, d, ³J_{HH} = 7.5 Hz), 7.10 (2H, app. t, ³J_{HH} = 7.4 Hz), 7.00 (2H, app. t, ³J_{HH} = 7.5 Hz), 6.47 (2H, t, ³J_{HH} = 6.9 Hz), 4.17 (4H, q, ³J_{HH} = 7.1 Hz, OCH₂CH₂OCH₃), 3.53-3.49 (4H, m, OCH₂CH₂OCH₃), 3.32 (6H, s, OCH₃), 1.51 (6H, s, CH₃) ppm. LRMS (ES⁺) found *m/z* 1043.20; calculated 1042.21 for [M-PF₆]⁺. HRMS (ES⁺) found *m/z* 1043.1833; calculated 1043.2105 for [C₄₆H₄₀N₇O₆S₂Ir]⁺. IR (solid): ν 1716 (C=O), 1256, 1230 (C-O), 837 (PF₆⁻) cm⁻¹.

[Ir(emptz)₂(ppiphen)]PF₆

As for [Ir(emptz)₂(bpy)]PF₆, but using **1** (0.060 g, 0.04 mmol) and **ppiphen** (0.029 g, 0.08 mmol). The crude product was purified by column chromatography (silica, CH₂Cl₂). After elution of unreacted organics with CH₂Cl₂ the product was eluted as the third orange fraction with CH₂Cl₂/MeOH (9:1). Yield:

0.021 g, 20%. ¹H NMR (400 MHz, CDCl₃): δ_H = 9.29-9.28 (1H, m), 8.54 (2H, app. dd, *J*_{HH} = 4.6, 1.6 Hz), 7.71 (2H, dd, *J*_{HH} = 7.6, 2.0 Hz), 7.68 (1H, d, ³J_{HH} = 1.1 Hz), 7.65-7.63 (9H, m), 7.44-7.43 (2H, m), 7.08 (2H, d, ³J_{HH} = 7.7 Hz), 6.98-6.97 (2H, d, ³J_{HH} = 7.5 Hz), 6.49-6.41 (2H, m), 4.27-4.26 (4H, m, OCH₂CH₂OCH₃), 3.55-3.53 (4H, m, OCH₂CH₂OCH₃), 3.27 (6H, s, OCH₃), 1.53 (6H, s, CH₃) ppm. UV/Vis (CH₃CN): λ_{max}/nm (ε/M⁻¹cm⁻¹) = 439 (8600), 397 (9000), 371 (11900), 282 (66700). LRMS (ES⁺) found *m/z* 1118.25; calculated 1118.31 for [M-PF₆]⁺. HRMS (ES⁺) found *m/z* 1118.2328; calculated 1118.2341 for [C₅₂H₄₃N₇O₆S₂Ir]⁺. IR (solid): ν 1716 (C=O), 1257, 1242 (C-O), 833 (PF₆⁻) cm⁻¹.

[Ir(emptz)₂(bpiphen)]PF₆

As for [Ir(emptz)₂(bpy)]PF₆, but using **1** (0.055 g, 0.04 mmol) and **bpiphen** (0.032 g, 0.07 mmol). The crude product was purified by column chromatography (silica, CH₂Cl₂). After elution of unreacted organics with CH₂Cl₂ the product was eluted as the second orange fraction with CH₂Cl₂/MeOH (9:1). Yield: 0.016 g, 17%. ¹H NMR (400 MHz, CDCl₃): δ_H = 9.26 (1H, dd, *J*_{HH} = 8.2, 1.5 Hz), 8.53-8.52 (2H, m), 8.16 (1H, dd, *J*_{HH} = 5.3, 1.5 Hz), 8.08 (1H, dd, *J*_{HH} = 5.1, 1.3 Hz), 7.83 (1H, dd, *J*_{HH} = 8.2, 5.3 Hz), 7.74-7.65 (5H, m), 7.56 (1H, dd, *J*_{HH} = 8.6, 5.1 Hz), 7.49-7.45 (2H, m), 7.41 (2H, dd, *J*_{HH} = 4.7, 1.8 Hz), 7.10-7.05 (2H, m), 6.99-6.94 (2H, m), 6.46 (2H, dd, *J*_{HH} = 17.8, 7.3 Hz), 4.18 (4H, q, ³J_{HH} = 3.6 Hz, OCH₂CH₃), 1.52 (6H, s, CH₃), 1.37 (9H, s, CH₃), 1.26-1.19 (6H, m, OCH₂CH₃) ppm. UV/Vis (CH₃CN): λ_{max}/nm (ε/M⁻¹cm⁻¹) = 440 (8600), 398 (9200), 371 (12100), 282 (71200). LRMS (ES⁺) found *m/z* 1114.41; calculated 1114.37 for [M-PF₆]⁺. HRMS (ES⁺) found *m/z* 1114.2743; calculated 1114.2745 for [C₅₄H₄₇N₇S₂O₄Ir]⁺. IR (solid): ν 1716 (C=O), 1244, 1233 (C-O), 837 (PF₆⁻) cm⁻¹.

Conclusions

This paper describes the synthesis, structural and spectroscopic properties of a range of cationic Ir(III) complexes that incorporate cyclometalated substituted 2-phenylthiazole ligands. The complexes are phosphorescent with an emitting state that appears to have some mixed ³MLCT and ³IL character. The precise nature of the ancillary N[^]N ligand influences the observed lifetimes: the introduction of dppz-type ligands partially quenches the emitting state, probably *via* low-lying ligand-centred states localised on the dppz moiety.

Further work is possible with these complexes. We have previously shown that the introduction of ester groups onto the cyclometalated ligand is a viable route to water-soluble phosphorescent species;¹² such an approach will be investigated in the future with these complexes. The **piphen**, **ppiphen** and **bpiphen** derivatives also offer an additional pyridine coordination site, which will be investigated in the context of mixed metal assemblies. It is also noteworthy that previous reports have also shown that dppz complexes of Ir(III) can be used to investigate redox reactions of DNA.³⁶

Acknowledgements

We thank Cardiff University for financial support and the staff of the EPSRC Mass Spectrometry National Service (University of

Swansea) for providing MS data. We also thank the EPSRC for the use of the National Crystallographic Service at the University of Southampton.

Notes and references

⁵ ^a School of Chemistry, Main Building, Cardiff University, Cardiff CF10 3AT. Fax: (+44) 029-20874030; Tel: (+44) 029-20879316; E-mail: popesj@cardiff.ac.uk; UK National Crystallographic Service, Chemistry, Faculty of Natural and Environmental Sciences, University of Southampton, Highfield, Southampton, SO17 1BJ, England, UK

¹⁰ † Electronic Supplementary Information (ESI) available: data collection parameters for both crystallographic studies, pictorial representations of the calculated frontier orbitals for $[\text{Ir}(\text{emtpz})_2(\text{phen})]^+$, examples of cyclic voltammograms and experimental data for the ligands. See DOI: 10.1039/b000000x/

¹ a) S. Ladouceur, E. Zysman-Colman, *Eur. J. Inorg. Chem.*, 2013, 2985; b) A. Ruggi, F.W.B. van Leeuwen, A.H. Velders, *Coord. Chem. Rev.*, 2011, 255, 2542; c) K. K-W. Lo, M-W. Louie, K.Y. Zhang, *Coord. Chem. Rev.*, 2010, 254, 2603.

² a) J. D. Slinker, A. A. Gorodetsky, M. S. Lowry, J. J. Wang, S. Parker, R. Rohl, S. Bernhardt and G. G. Malliaras, *J. Am. Chem. Soc.*, 2004, **126**, 2763; b) S. Evariste, M. Sandroni, T. Rees, C. Roldan-Carmona, L. Gil-Escrig, H. Bolink, E. Baranoff, E. Zysman-Colman, *J. Mater. Chem. C.*, 2014, **2**, 5793; c) J. M. Fernandez-Hernandez, S. Ladouceur, Y. Shen, A. Iordache, X. Wang, L. Donato, S. Gallagher-Duval, M. de Anda Villa, J. D. Slinker, L. De Cola, E. Zysman-Colman, *J. Mater. Chem. C.*, 2013, **1**, 7440.

³ a) J. I. Goldsmith, W. R. Hudson, M. S. Lowry, T. H. Anderson, S. Bernhard, *J. Am. Chem. Soc.*, 2005, **127**, 7502; b) S. Takizawa, R. Aboshi, S. Murata, *Photochem. Photobiol. Sci.*, 2011, **10**, 895; c) Y.-J. Yuan, J.-Y. Zhang, Z.-T. Yu, J.-Y. Feng, W.-J. Luo, J.-H. Ye, Z.-G. Zou, *Inorg. Chem.*, 2012, **51**, 4123; d) A. J. Hallett, N. White, W. Wu, X. Cui, P. N. Horton, S. J. Coles, J. Zhao, S. J. A. Pope, *Chem. Commun.*, 2012, **48**, 10838; e) J. Sun, F. Zhong, X. Yi, J. Zhao, *Inorg. Chem.*, 2013, **52**, 6299.

⁴ For example, a) W. H.-T. Law, L. C.-C. Lee, M.-W. Louie, H.-W. Liu, T. W.-H. Ang and K. K.-W. Lo, *Inorg. Chem.*, 2013, **52**, 13029; b) B. Wang, Y. Liang, H. Dong, T. Tan, B. Zhan, J. Cheng, K. K. W. Lo, Y. W. Lam and S. H. Cheng, *ChemBioChem*, 2012, **13**, 2729; c) S. P. Y. Li, T. S.-M. Tang, K. S.-M. Yiu and K. K. W. Lo, *Chem. Eur. J.*, 2012, **18**, 13342;

⁵ G.-G. Shan, H.-B. Li, H.-T. Cao, D.-X. Zhu, P. Li, Z.-M. Su, Y. Liao, *Chem. Commun.*, 2012, **48**, 2000.

⁶ H. Sun, S. Liu, W. Lin, K. Y. Zhang, W. Lv, X. Huang, F. Huo, H. Yang, G. Jenkins, Q. Zhao, W. Huang, *Nat. Commun.*, 2014, **5**, 3601.

⁷ a) I. Avilov, P. Minoofar, J. Cornil, L. De Cola, *J. Am. Chem. Soc.*, 2007, **129**, 8247; b) A. Ruggi, M. Mauro, F. Polo, D. N. Reinhoudt, L. De Cola, A. H. Velders, *Eur. J. Inorg. Chem.*, 2012, 1025; c) S. Ladouceur, D. Fortin, E. Zysman-Colman, *Inorg. Chem.*, 2010, **49**, 5625; d) E. Baranoff, I. Jung, R. Scopelliti, E. Solari, M. Gratzel, M. K. Nazeeruddin, *Dalton Trans.*, 2011, **40**, 6860.

⁸ a) K. Hanson, L. Roskop, P. I. Djurovich, F. Zahariev, M. S. Gordon, M.E. Thompson, *J. Am. Chem. Soc.*, 2010, **132**, 16247; b) D. Sykes, I. S. Tidmarsh, A. Barbieri, I. V. Sazanovich, J. A. Weinstein, M. D. Ward, *Inorg. Chem.*, 2011, **50**, 11323; c) D. L. Davies, M. P. Lowe, K. S. Ryder, K. Singh, S. Singh, *Dalton Trans.*, 2011, **40**, 1028

⁹ For example, a) R. Gao, D. G. Ho, B. Hernandez, M. Selke, D. Murphy, P. I. Djurovich, M. E. Thompson, *J. Am. Chem. Soc.*, 2002, **124**, 14828; b) R. Wang, D. Liu, H. Ren, T. Zhang, X. Wang, J. Li, *J. Mater. Chem.*, 2011, **21**, 15494; c) I. R. Laskar, T.-M. Chen, *Chem. Mater.*, 2004, **16**, 111.

¹⁰ a) X. Yang, Y. Zhao, X. Zhang, R. Li, J. Dang, Y. Li, G. Zhou, Z. Wu, D. Ma, W.-Y. Wong, X. Zhao, A. Ren, L. Wang, X. Hou, *J. Mater. Chem.*, 2012, **22**, 7136; b) F. Gartner, S. Denurra, S. Losse, A. Neubauer, A. Boddien, A. Gopinathan, A. Spannenberg, H. Junge, S.

Lochbrunner, M. Blug, S. Hoch, J. Busse, S. Gladiali, M. Beller, *Chem. Eur. J.*, 2012, **18**, 3220; c) C. Yao, B. Jiao, X. Yang, X. Xu, J. Dang, G. Zhou, Z. Wu, X. Lv, Y. Zeng, W.-Y. Wong, *Eur. J. Inorg. Chem.*, 2013, 4754; d) X. Xu, Y. Zhao, J. Dang, X. Yang, G. Zhou, D. Ma, L. Wang, W.-Y. Wong, Z. Wu, X. Zhao, *Eur. J. Inorg. Chem.*, 2012, 2278; e) M. Xu, R. Zhou, G. Wang, J. Yu, *Inorg. Chim. Acta*, 2009, **362**, 515.

¹¹ a) E. E. Langdon-Jones, A. J. Hallett, J. D. Routledge, D. A. Crole, B. D. Ward, J. A. Platts, S. J. A. Pope, *Inorg. Chem.*, 2013, **52**, 448; b) J. D. Routledge, A. J. Hallett, J. A. Platts, P. N. Horton, S. J. Coles, S. J. A. Pope, *Eur. J. Inorg. Chem.*, 2012, 4065.

¹² R. A. Smith, E. C. Stokes, E. E. Langdon-Jones, J. A. Platts, B. M. Kariuki, A. J. Hallett, S. J. A. Pope, *Dalton Trans.*, 2013, **42**, 10347.

¹³ F. Shao, B. Elias, W. Lu, J.K. Barton, *Inorg. Chem.*, 2007, **46**, 10187.

¹⁴ N. N. Sergeeva, M. Donnier-Marechal, G. Vaz, A. M. Davies, M. O. Senge, *J. Inorg. Biochem.*, 2011, **105**, 1589.

¹⁵ M. Nonoyama, *Bull. Chem. Soc. Jpn.*, 1974, **47**, 767.

¹⁶ K. Dedeian, P. I. Djurovich, F. O. Garces, G. Carlson, R. J. Watts, *Inorg. Chem.*, 1991, **30**, 1685.

¹⁷ K. A. King, R. J. Watts, *J. Am. Chem. Soc.*, 1987, **109**, 1589.

¹⁸ V.V. Pavlishchuk, A.W. Addison, *Inorg. Chim. Acta*, 2000, **298**, 97.

¹⁹ S. Ladouceur, D. Fortin, E. Zysman-Colman, *Inorg. Chem.*, 2011, **50**, 11514.

²⁰ J. Dyer, W. J. Blau, C. G. Coates, C. M. Creely, J. D. Gavey, M. W. George, D. C. Grills, S. Hudson, J. M. Kelly, P. Matousek, J. J. McGarvey, J. McMaster, A. W. Parker, M. Towrie, J. A. Weinstein, *Photochem. Photobiol. Sci.*, 2003, **2**, 542.

²¹ N. G. Connelly and W. E. Geiger, *Chem. Rev.*, 1996, **96**, 877.

²² S. J. Coles, P. A. Gale, *Chem. Sci.*, 2012, **3**, 683

²³ *CrystalClear-SM Expert 3.1 b27*, 2013, Rigaku

²⁴ L. Palatinus, G. Chapuis, *J. Appl. Cryst.*, 2007, **40**, 786.

²⁵ G.M. Sheldrick, *Acta Cryst.*, 2008, **A64**, 112.

²⁶ M. J. Frisch, G. W. Trucks, H. B. Schlegel, G. E. Scuseria, M. A. Robb, J. R. Cheeseman, J. A. Montgomery Jr., T. Vreven, K. N. Kudin, J. C. Burant, J. M. Millam, S. S. Iyengar, J. Tomasi, V. Barone, B. Mennucci, M. Cossi, G. Scalmani, N. Rega, G. A. Petersson, H. Nakatsuji, M. Hada, M. Ehara, K. Toyota, R. Fukuda, J. Hasegawa, M. Ishida, T. Nakajima, Y. Honda, O. Kitao, H. Nakai, M. Klene, X. Li, J. E. Knox, H. P. Hratchian, J. B. Cross, V. Bakken, C. Adamo, J. Jaramillo, R. Gomperts, R. E. Stratmann, O. Yazyev, A. J. Austin, R. Cammi, C. Pomelli, J. W. Ochterski, P. Y. Ayala, K. Morokuma, G. A. Voth, P. Salvador, J. J. Dannenberg, V. G. Zakrzewski, S. Dapprich, A. D. Daniels, M. C. Strain, O. Farkas, D. K. Malick, A. D. Rabuck, K. Raghavachari, J. B. Foresman, J. V. Ortiz, Q. Cui, A. G. Baboul, S. Clifford, J. Cioslowski, B. B. Stefanov, G. Liu, A. Liashenko, P. Piskorz, I. Komaromi, R. L. Martin, D. J. Fox, T. Keith, M. A. Al-Laham, C. Y. Peng, A. Nanayakkara, M. Challacombe, P. M. W. Gill, B. Johnson, W. Chen, M. W. Wong, C. Gonzalez, J. A. Pople, Gaussian 03, Revision E.01. Gaussian, Inc., Wallingford CT, 2004.

²⁷ (a) P. J. Hay, W. R. Wadt, *J. Chem. Phys.*, 1985, **82**, 270. (b) P. J. Hay and W. R. Wadt, *J. Chem. Phys.* 1985, **82**, 299.

²⁸ (a) M. M. Francl, W. J. Pietro, W. J. Hehre, J. S. Binkley, D. J. DeFrees, J. A. Pople and M. S. Gordon, *J. Chem. Phys.*, 1982, **77**, 3654. (b) P. C. Hariharan and J. A. Pople, *Theor. Chem. Acc.*, 1973, **28**, 213.

²⁹ Gaussian 09, Revision C.01, M. J. Frisch, G. W. Trucks, H. B. Schlegel, G. E. Scuseria, M. A. Robb, J. R. Cheeseman, G. Scalmani, V. Barone, B. Mennucci, G. A. Petersson, H. Nakatsuji, M. Caricato, X. Li, H. P. Hratchian, A. F. Izmaylov, J. Bloino, G. Zheng, J. L. Sonnenberg, M. Hada, M. Ehara, K. Toyota, R. Fukuda, J. Hasegawa, M. Ishida, T. Nakajima, Y. Honda, O. Kitao, H. Nakai, T. Vreven, J. A. Montgomery, Jr., J. E. Peralta, F. Ogliaro, M. Bearpark, J. J. Heyd, E. Brothers, K. N. Kudin, V. N. Staroverov, T. Keith, R. Kobayashi, J. Normand, K. Raghavachari, A. Rendell, J. C. Burant, S. S. Iyengar, J. Tomasi, M. Cossi, N. Rega, J. M. Millam, M. Klene, J. E. Knox, J. B. Cross, V. Bakken, C. Adamo, J. Jaramillo, R. Gomperts, R. E. Stratmann, O. Yazyev, A. J. Austin, R. Cammi, C.

-
- Pomelli, J. W. Ochterski, R. L. Martin, K. Morokuma, V. G. Zakrzewski, G. A. Voth, P. Salvador, J. J. Dannenberg, S. Dapprich, A. D. Daniels, O. Farkas, J. B. Foresman, J. V. Ortiz, J. Cioslowski, and D. J. Fox, Gaussian, Inc., Wallingford CT, 2010.
- ³⁰ J. Tomasi, B. Mennucci, R. Cammi, *Chem. Rev.*, 2005, **105**, 2999 and references therein.
- ³¹ G. Li, Y. He, W. Zhou, P. Wang, Y. Zhang, W. Tong, H. Wu, M. Liu, X. Ye, Y. Chen, *Heterocycles*, 2014, **89**, 453.
- ³² R. Satapathy, H. Padhy, Y-H. Wu, H-C. Lin, *Chem. Eur. J.*, 2012, **18**, 16061.
- ³³ D. S. Beaudoin, S. O. Obare, *Tetrahedron Lett.*, 2008, **49**, 6023.
- ³⁴ I Katsuyama, M. Kubo, *Heterocycles*, 2007, **71**, 2491.
- ³⁵ N. J. Lundin, P. J. Walsh, S. L. Howell, J. J. McGarvey, A. G. Blackman, K. C. Gordon, *Inorg. Chem.*, 2005, **44**, 3551.
- ³⁶ F. Shao, J. K. Barton, *J. Am. Chem. Soc.*, 2007, **129**, 14733.

TOC entry

Ten cationic heteroleptic iridium(III) complexes involving substituted phenylthiazole ligands reveal phosphorescence emission in solution.

